Organic Electronics 109 (2022) 106622

Contents lists available at ScienceDirect

Organic Electronics

journal homepage: www.elsevier.com/locate/orgel

A synaptic memristor based on natural organic honey with neural facilitation

Brandon Sueoka [a,1], Md Mehedi Hasan Tanim [a,1], Lauren Williams [b], Zhigang Xiao [b], Ying Zhi Seah [c], Kuan Yew Cheong [c,**], Feng Zhao [a,*]

[a] Micro/Nanoelectronic and Energy Laboratory, School of Engineering and Computer Science, Washington State University, Vancouver, WA, 98686, United States
[b] Department of Electrical Engineering, Alabama A&M University, Normal, AL, 35762, United States
[c] School of Materials and Mineral Resources Engineering, Engineering Campus, Universiti Sains Malaysia, 14300, Nibong Tebal, Penang, Malaysia

ARTICLE INFO

Keywords:
Honey
Natural organic material
Artificial synaptic device
Neural facilitation
Paired-pulse facilitation index
Neuromorphic computing

ABSTRACT

Neural facilitation is an essential activity-dependent synaptic plasticity in most chemically transmitting synapses. Emerging artificial synaptic devices need to be capable of emulating this function in order to be used in brain-inspired neuromorphic computing systems. In this paper, neural facilitation in natural organic honey based synaptic memristor was investigated. The memristive layer was fabricated by commercially purchased honey via a solution-based process and sandwiched in between Al top electrode and ITO bottom electrode. Two process conditions, 90 °C/8 h and 140 °C/2 h were applied to dry the honey thin film for comparison. Test results show that both devices demonstrated bipolar resistive switching and neural facilitation behaviors, while the memristor with the honey film dried by 90 °C/8 h demonstrated a larger on/off ratio and read memory window, lower current at high-resistant state, and larger facilitation index. The index is also larger than our previously reported honey-memristor with same drying conditions but Ag top electrode, and memristors based on other natural organic materials such as chicken albumen and lignin. The index decayed following two exponential phases as a function of the interval time of the two stimulation voltage pulses, which is similar to biological synapses. Besides shorter pulse interval time, the response of facilitation also enhanced by larger magnitude and width of the stimulation voltage pulses.

1. Introduction

Functional emulation of biological synapse by artificial synaptic devices is critical for the development of brain-inspired neuromorphic systems which overcome the energy consumption challenge faced by conventional computing based on von Neumann architecture. One promising device technology proven to be capable of emulating synaptic functions is resistive switching memristor because of its tunable resistance, scalability, nonvolatility, high data retention capability and good endurance, CMOS and 3D integration compatibility, multistate programmability, low power consumption, and relatively high speed [1–5]. These merits enable resistive switching memristor to be a desirable candidate for data storage, data transmission, memory logic, and neuromorphic computing systems [6–8]. Synaptic memristor is a nonlinear two-terminal device with a dielectric thin film sandwiched between two electrodes. The dielectric thin film is the critical layer responsible for resistive switching and tunable resistance of the device. Such device structure resembles "point-to-point" connected biological synapses. Natural organic materials have attracted interest to form such resistive switching films because they are renewable, biodegradable, sustainable, biocompatible, and environmentally friendly. So far various artificial synaptic devices with resistive switching layer based on natural organic materials [9–15] have been developed as desirable candidates for "green" neuromorphic systems.

In our previous studies [14,15], we have reported synaptic memristors with commercial honey fabricated into the resistive switching film by a solution process to emulate synaptic plasticity of biological synapse. Honey is a mixture containing more than 180 constituents [16], mainly sugar, which is represented by about 75% monosaccharides (glucose and fructose), followed by 10–15% disaccharides (sucrose,

* Corresponding author.
** Corresponding author.
E-mail addresses: srcheong@usm.my (K.Y. Cheong), feng.zhao@wsu.edu (F. Zhao).
[1] Equal contribution.

https://doi.org/10.1016/j.orgel.2022.106622
Received 2 July 2022; Received in revised form 3 August 2022; Accepted 3 August 2022
Available online 7 August 2022

maltose, turanose, isomaltose, etc.) and small amount of trisaccharides (maltotriose and melezitose). Neural facilitation, also known as paired-pulse facilitation (PPF), is a form of short-term, activity-dependent synaptic plasticity common to most chemically transmitting synapses [17]. It describes the phenomenon that the second of two rapidly and closely evoked excitatory postsynaptic potentials (EPSPs) has larger amplitude. Neural facilitation is important for neural tasks in brain such as learning, information and cognitive processing. We have demonstrated neural facilitation in honey-memristor with Ag top electrode and ITO bottom electrode, i.e. Ag/honey/ITO [15]. It is known that electrode materials and dielectric film process parameters affect the resistive switching characteristics, while in this study we investigated these effects on the synaptic properties with focus on the neural facilitation. Two honey-memristor devices were fabricated with same Al top electrode and ITO bottom electrode (Al/honey/ITO) but different drying temperatures and durations for honey films, i.e. 90 °C for 8 h and 140 °C for 2 h. The results from this study can be used for selection of potential artificial synaptic devices for future renewable and biodegradable neuromorphic computing systems.

2. Experimental

Honey-memristors under investigation were fabricated on two 2.5 cm × 2.5 cm glass slides. Both glass slides were cleaned by acetone, isopropyl alcohol and D.I. water in an ultrasonic bath for 10 min each. After cleaning, they were loaded in a Nano 36 DC/RF sputter (Kurt J. Lesker) for ITO thin film deposition to form bottom electrode. The final sheet resistance of ITO film was 10 Ω/sq. Commercial honey was mixed with D.I. water for a 30% concentration by weight. The honey solution was coated on the ITO/glass substrates at 1000 rpm for 90 s on a spinner, followed by baking on a hotplate in air to dry the honey films. One sample was baked at 90 °C for 8 h and denoted as Al/honey/ITO (90:8), and the other sample at 140 °C for 2 h as Al/honey/ITO (140:2). After baking, each sample was covered by a stencil mask with circular windows for a deposition of 100 nm-thick Al film on the dried honey film by e-beam evaporation (PVD 75 e-beam/thermal evaporation system, Kurt J. Lesker to form top Al electrode arrays. Schematic process flow of honey memristors and a photograph after fabrication are shown in Fig. 1 (a) and (b).

Electrical measurements on resistive switching and PPF characterization were performed on a probe-station at room temperature in air using a Keithley 4200 semiconductor characterization system, a Tektronix AFG 310 arbitrary function generator and a Tektronix DPO 2024 oscilloscope. The schematic test circuit diagram is shown in Fig. 1(c). A pair of voltage pulses was applied by the function generator on the Al top electrode of the honey-memristor while the ITO bottom electrode was grounded. The corresponding current in the honey-memristor was calculated from the voltage drop measured by the oscilloscope on a 2000 Ω resistor connected in series with the honey-memristor. Thermal analysis of the honey solution was tested via a differential scanning calorimetry (DSC, PerkinElmer DSC 4000, Pyris 6) from 30 to 200 °C under N_2 ambient with a flow rate of 20 ml/min and heating rate of 5 °C/min. Attenuated total reflection mode Fourier transform infrared spectroscopy (ATR-FTIR) (Bruker alpha Eco-ATRIR with ZnSe crystal) was used to determine chemical functional groups of dried honey thin films.

3. Results and discussion

Resistive switching properties of honey-memristors were first verified. Fig. 2(a) presents a family plot of typical current-voltage (I–V) characteristics. DC voltage sweeping rate was 1 V/s and the voltage sweep sequence was numbered in the plot. It was shown that both devices demonstrated bipolar resistive switching characteristics without initial forming process. The high resistance state (HRS) currents in both devices change gradually by more than 3–4 orders of magnitude before SET and RESET process, which is similar to our previously reported Ag/honey/ITO [12] and Cu/honey/Cu_xO [14] memristors. Such switching characteristics are essential for memristors to emulate synaptic plasticity. It is clearly noted that the on/off ratios, read memory windows, and high-resistance state currents were different in both devices. Both SET and RESET voltages and therefore the read memory window of the Al/honey/ITO (90:8) device were much larger than those of the Al/honey/ITO (140:2) device, while HRS current of Al/honey/ITO (90:8) was much lower than that of Al/honey/ITO (140:2) device.

To examine the data endurance, honey-memristors from both samples were switched for 200 consecutive cycles. The cumulative probability of SET and RESET voltages is shown in Fig. 2(b), which demonstrated uniformity with a narrow 1 V range in most probabilities. The data retention characteristics at HRS and low resistance state (LRS) under a continuous voltage stress for 10^4 s at respective read voltages of two honey-memristors are shown in Fig. 2(c). The retention time test was performed in air and at room temperature. Currents in both honey-memristors were retained over the time period of 10^4 s and no significant degradation was observed even when the retention time was extrapolated to 10 years. These characteristics showed that these honey-memristors has good cycle-to-cycle and device-to-device stability and reliable data retention for non-volatile memory applications.

The different values of on/off ratios, read memory windows, and

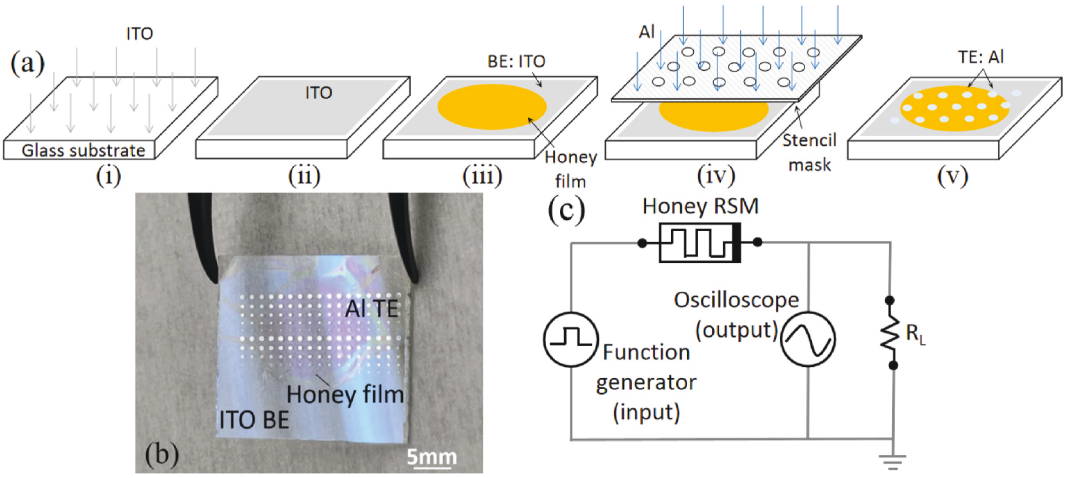

Fig. 1. (a) Schematic process flow of Al/honey/ITO synaptic memristor: (i) deposition of ITO on glass substrate, (ii) after ITO deposition, (iii) spin coating and baking honey film on ITO bottom electrode (BE), (iv) deposition of Al top electrode (BE) through a stencil mask, (v) finished devices. (b) Photographs of honey-memristors. (c) Schematic test circuit diagram for PPF characterizations.

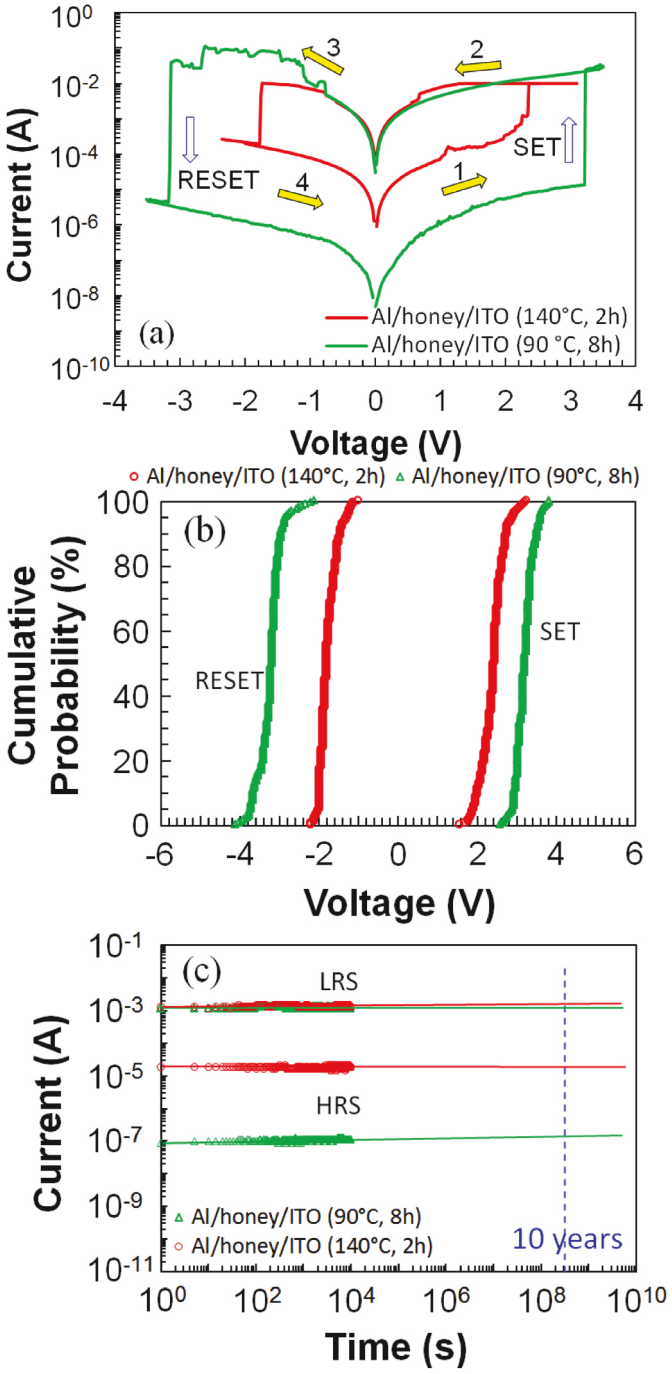

Fig. 2. (a) Bipolar resistive switching characteristics of Al/honey/ITO memristors. Voltage sweep sequence was numbered. Devices were in HRS during voltage sweep 1 and 4, and in LRS during voltage sweep 2 and 3. (b) Switching endurance measured for 200 cycles with cumulative probability distribution of SET and RESET voltages. (c) Data retention for 10^4 s.

high-resistance state currents are attributed to the different chemical drying temperatures, 90 °C versus 140 °C, of the honey films. Based on DSC results in Fig. 3(a), the honey thin film was not fully solidified when dried at 90 °C if compared with its counterpart dried at 140 °C. Substantial amount of –OH group (~3200 cm^{-1}) can be detected by ATR-FTIR in honey film dried at 90 °C, but this chemical functional group was completely undetectable in the film dried at a 140 °C, as shown in Fig. 3(b). The –OH group originated from either water and/or polysaccharides compounds in honey such as glucose, fructose, sucrose, etc. However, C–O group (1050 cm^{-1}) for honey dried at 140 °C increased

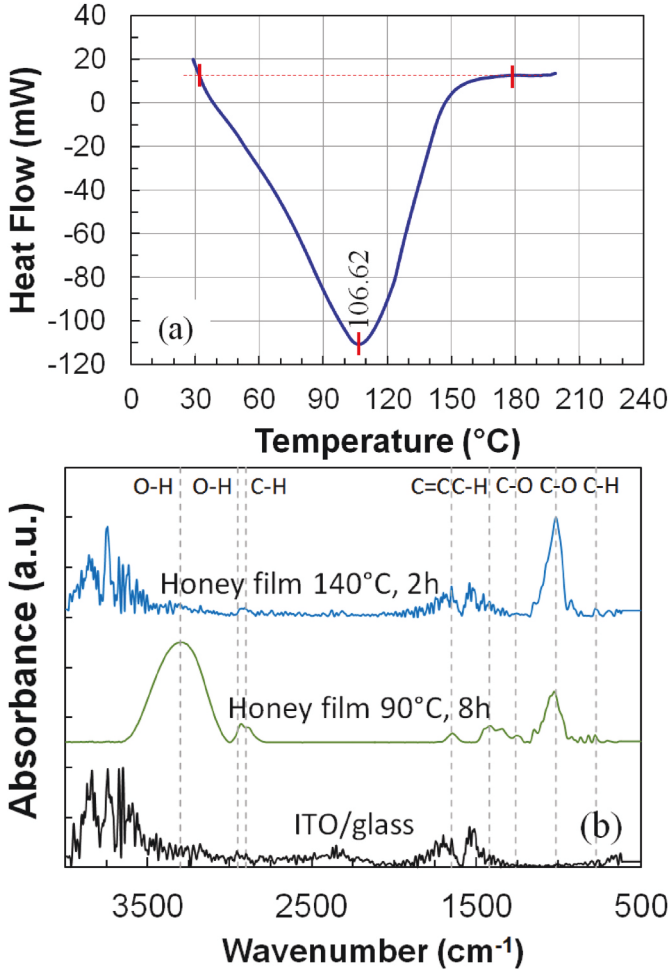

Fig. 3. (a) Change of heat flow of honey solution measured by DSC. (b) Comparison of absorbance spectra obtained from ATR-FTIR for bare ITO/glass substrate and dried honey thin films at 90 °C and 140 °C.

significantly. This is the main chemical functional group of monosaccharides compounds dissociated from polysaccharides of honey. As higher drying temperature was applied, higher amount of short chain monosaccharides was contained in the honey film. Insulating property of the honey thin film is more obvious with higher amount of –OH group, corresponding to the higher resistance when the honey film is dried at 90 °C than 140 °C; therefore, its HRS current is lower and a higher voltage is needed to switch from HRS to LRS. –OH group may not contribute much once the memory was switched to LRS as the current level at LRS state was comparable in both devices. Based on these results, it is also proven that –OH group is more dominating than C–O group for controlling the resistive switching behavior in honey-memristors.

To identify the current conduction mechanism, I–V curves in Fig. 2 (a) were replotted in log-log scale with linear fittings as shown in Fig. 4 (a). In HRS, two distinct slopes were observed in Al/honey/ITO (90:8) device, indicating the typical space charge limited conduction (SCLC) [18]. At low voltages, the linear (slope ≈ 1) I–V curves follow Ohm's law while at high voltages, they change to quadratic (slope ≈ 2) by Mott--Gurney's law of trap-free limitation. In LRS, Al/honey/ITO (90:8) device showed linear I–V curves across the whole voltage range, suggesting metallic filamentary conduction based on Ohm's law. For Al/honey/ITO (140:2) device, linear I–V curves were observed in both HRS and LRS, indicating that current conduction is dominated by Ohm's law.

The resistive switching mechanisms are schematically presented in Fig. 4(b ~ d and b'~d'). In HRS and low voltage, due to the positive bias

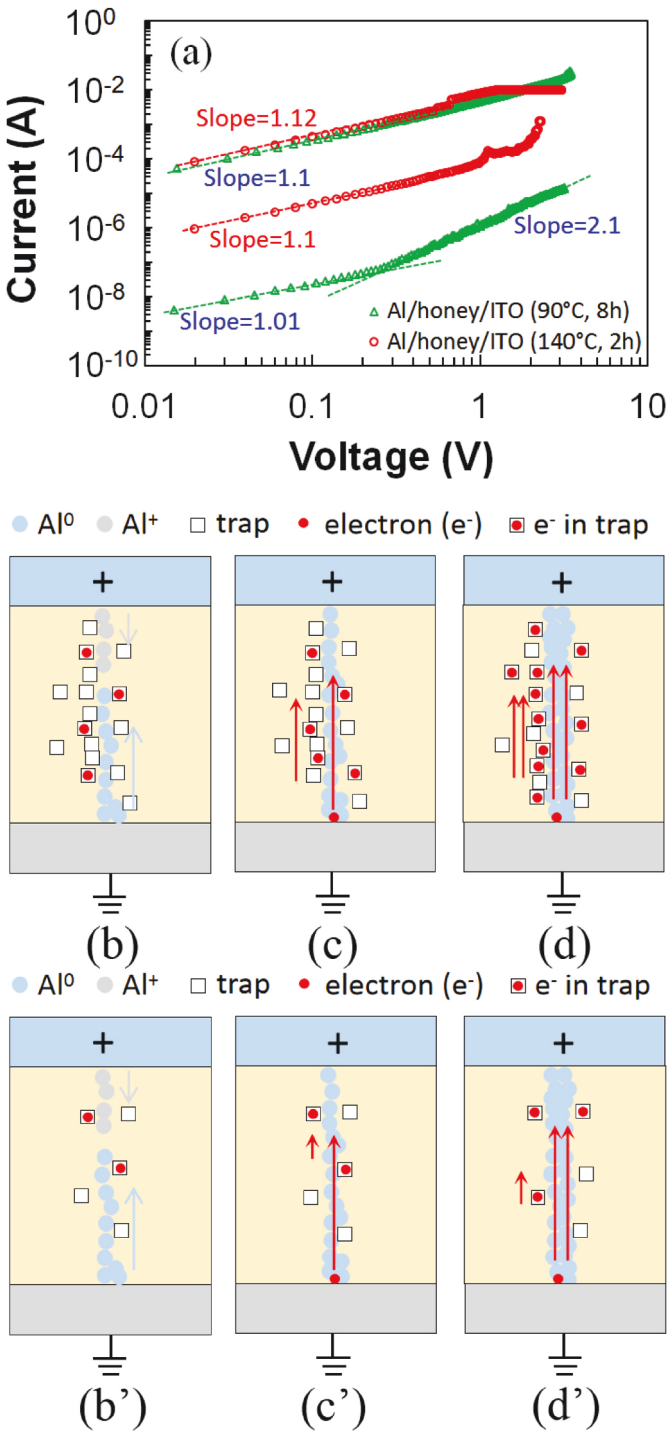

Fig. 4. (a) Resistive switching I–V curves in Fig. 2(a) were replotted in log-log scale. Schematic of resistive switching in (b ~ d) Al/honey/ITO (90 °C, 8 h) and (b'~d') Al/honey/ITO (140 °C, 2 h) devices. (b, b') At a low voltage; (c, c') approaching SET voltage; (d, d') at SET voltage.

on the top Al electrode, Al atom (Al^0) was oxidized to Al ion (Al^+) and drifted along the bulk honey film toward the bottom ITO electrode. When reaching the bottom electrode, Al^+ was reduced to Al^0 and Al atoms stacked from the bottom electrode to form Al filaments toward the top electrode [Fig. 4(b and b')]. Trap centers due to structural arrangement of functional –OH groups (deep traps) and structural defects due to baking (shallow traps) also existed in the honey film and captured electrons, and more trap centers presented in the honey film baked at 90 °C for 8 h than at 140 °C for 2 h as compared in Fig. 4(b and b'). When the bias voltage was approaching the SET voltage, higher energy and mobility allowed the filled electrons to escape from trap centers and transport along both traps and Al filaments, with the current increasing in the memristor. The large density of trap centers released more electrons, resulting in an increased current slope from 1 to 2.1 in the Al/honey/ITO (90:8) device [Fig. 4(c)]. The unit slope was maintained in the Al/honey/ITO (140:2) device due to the low density of trap centers in which the electrons in filaments dominated the current conduction [Fig. 4(c')]. At SET voltage, more filaments were formed and more electrons transported along the filaments and trap centers, with current increasing abruptly and device transiting from HRS to LRS [Fig. 4(d and d')]. The correlation between the density of trap centers and baking condition is currently under investigation.

Honey-memristor can be regarded as a biological synapse as shown in Fig. 5. The top electrode, honey film and bottom electrode resemble the presynaptic neuron, synaptic cleft and postsynaptic neuron, respectively. In the current conduction process, Al ions resemble the neurotransmitters in the biological synapse. The current flow in honey-memristor emulated the excitatory postsynaptic current (EPSC) which is evoked by local stimulation in presynaptic neuron and recorded in postsynaptic neuron. Fig. 5 also shows schematically the PPF behavior of a biological synapse between a pre-synaptic neuron and a post-synaptic neuron, which is demonstrated by the enhancement in the amplitude of the second EPSC pulse than the first EPSC pulse in the postsynaptic neuron.

The responses of honey-memristor to temporally correlated signals were tested by stimulation with a pair of input voltage pulses of 3 V amplitude and 100 ms width with different time interval Δt. Fig. 6 (a) showed the PPF behavior of a Al/honey/ITO (90:8) device with Δt = 20 ms. The synaptic-PPF-like behavior of honey-memristor can be explained by the current conduction mechanism which is due to the conductive filaments [15,19]. Redox of the top metal electrode due to the application of the voltage pulse forms conductive filaments in the honey film for current conduction. It is believed that –OH group in honey plays an important role in the formation of the conductive filaments. When the second pulse was applied after the first pulse with a short interval time, additional conductive filaments were formed to further reduce the resistance of the honey film between the top and bottom electrode, which led to a higher current magnitude than that of the first pulse.

The ratio of the absolute amplitudes of the first and second current spike, i.e. PPF index (I_2/I_1), is used to quantify the PPF effect. Fig. 6(b) summarizes the PPF index with different interval time Δt from Al/honey/ITO (90:8) and Al/honey/ITO (140:2) devices. When Δt reduces, a larger PPF index can be obtained which represents a higher post-synaptic weight enhancement. This phenomenon is consistent with the trend observed in biological neurons [20,21]. It indicates that conductive filaments by the first voltage pulse were not strong for retention and could gradually rupture during the pulse interval, which suggests that the honey film returned to its original state when the pulse interval was long. In biological neurons, the PPF index can be modeled by a double exponential decay [22,23]:

$$PPF = c_1 e^{-\frac{\Delta t}{\tau_1}} + c_2 e^{-\frac{\Delta t}{\tau_2}} + 1 \quad (1)$$

where c_1 and c_2 are initial facilitation amplitude of the rapid phase and slow phase, and τ_1 and τ_2 are characteristic relaxation times of the rapid phase and slow phase, respectively. The PPF index modeled by Eq. (1) for both devices were plotted as the red and blue curves in Fig. 6(b), which fit the measurement results very well. As shown by the values of c_1, c_2, τ_1 and τ_2 in Fig. 6(b), the PFF index of both devices follow a fast phase (τ_1) with a higher amplitude (c_1), and a prolonged phase (τ_2) with a lower amplitude (c_2), which agrees with the biological synapses at the normal levels of extracellular calcium concentration $[Ca^{2+}]_e$ [24,25]. These values are close to those of other synaptic devices such as hybrid indium gallium zinc oxide (IGZO) synaptic transistor [26] and nickel

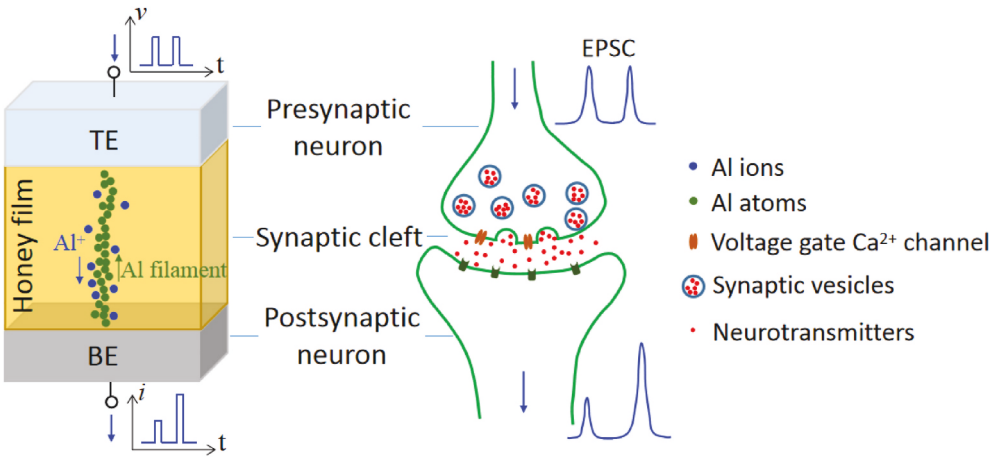

Fig. 5. Resemblance and PPF behaviors of biological synapse and honey-memristor. EPSC: excitatory postsynaptic currents.

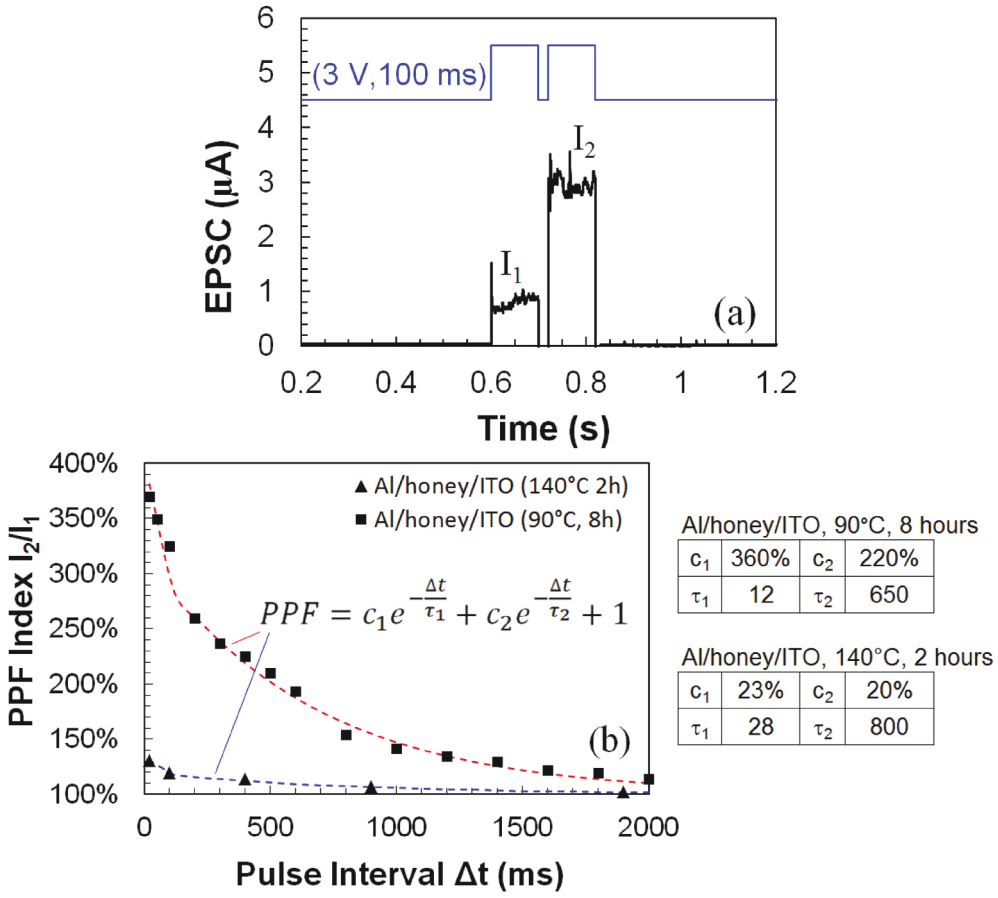

Fig. 6. (a) PPF behaviors of an Al/honey/ITO (90:8) memristor with postsynaptic EPSC triggered by a pair of presynaptic spikes with 20 ms interval times. (b) The PPF index of Al/honey/ITO (90:8) and Al/honey/ITO (140:2) devices as a function of inter-spike interval time. The red and blue curves represent the exponential fit modeled by Eq. (1).

oxide (NiO_x) based memristor [27].

Fig. 7 compares the PPF index measured from both Al/honey/ITO devices and in comparison with our previously reported Ag/honey/ITO memristor [12]. As can be observed, the PPF index was positive for all honey memristors under all pulse intervals. Among these three devices, our new Al/honey/ITO (90:8) memristor demonstrated much larger PPF index than other two devices at all interval times. Compared to Ag/honey/ITO, since honey films on both samples were dried at the same 90 °C for 8 h, the larger PPF index is attributed to the top metal electrode, Al over Ag. The PPF index of 370% by Al/honey/ITO (90:8) at 20 ms interval is also much higher than memristors based on other natural organic materials such as chicken albumen [28] and lignin [10]. The PPF index of Al/honey/ITO (140:2) showed lower PPF index at all intervals, indicating that baking temperature and duration also affect PPF, and baking at 140 °C for 2 h is not desirable for neural facilitation. A higher drying temperature indicates that the degradation of honey is more sever as disintegration of honey compounds may happen compared with lower drying temperature [Fig. 3(a)].

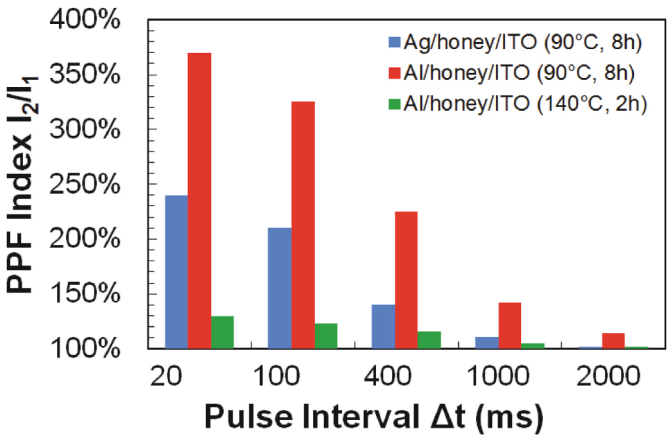

Fig. 7. Comparison of the PPF index of three honey based memristors as a function of inter-spike interval time.

Effects of the input pulse voltage magnitude and pulse width on PPF were also investigated. Al/honey/ITO (90:8) device was selected for this study with the pulse interval time fixed at 20 ms. Fig. 8(a) shows the PPF index as a function of the pulse voltage magnitude with a 100 ms pulse width. The results showed that the PPF index increased with the pulse voltage. Fig. 8(b) shows the PPF index as a function of the pulse width with the pulse voltage fixed at 3 V. The PPF index also increased from 120% when the pulse width was 20 ms–370% when the pulse width increased to 100 ms. Both higher voltage magnitude and longer pulse width can translate to more electrical energy applied in the honey film in both voltage stimuli, which formed more conductive filaments and strengthened existing filaments. This leads to a lower honey film resistance and therefore a larger current enhancement and PPF index.

In this work, only two honey drying temperatures (90 °C and 140 °C) and two top electrode materials (Al and Ag) were compared. According to DSC test results in Fig. 3(a), other drying temperatures could also affect the honey film quality and therefore the PPF index. In addition, the concentration of honey solution is also a very important parameter as the honey film was formed by a solution process, and in this study, only 30% concentration was applied. A comprehensive study on the effects of honey concentrations, drying temperature and duration, and top electrode materials on neural facilitation and PPF index is currently under investigation.

4. Conclusions

In this paper, neural facilitation behaviors of biological synapses were emulated by two synaptic memristors with Al top electrode, ITO bottom electrode, and honey thin film dried by two different conditions: 90 °C/8 h and 140 °C/2 h as the memristive layer. Both devices demonstrated bipolar resistive switching characteristics and neural facilitation properties, but Al/honey/ITO (90:8) has larger on/off ratio and read memory window, lower HRS currents and larger PPF index than those of Al/honey/ITO (140:2). The PPF index of this device is also larger than the previously reported Ag/honey/ITO memristor with the honey film dried at the same condition of 90 °C for 8 h, and memristors based on other natural organic materials such as chicken albumen and lignin. These results indicated that top electrode material and drying conditions affect the synaptic plasticity of honey-memristor. The dependence of PPF index on the pulse interval time showed a two-phase behavior which is similar to biological synapses. With two stimulation voltage pulses, the PPF index increased with reduced interval time but larger voltage magnitude and pulse width. Since natural organic honey has the advantages of renewable, sustainable, biodegradable, environmentally and biologically friendly, honey-based memristors are promising as hardware components for the development of renewable neuromorphic systems.

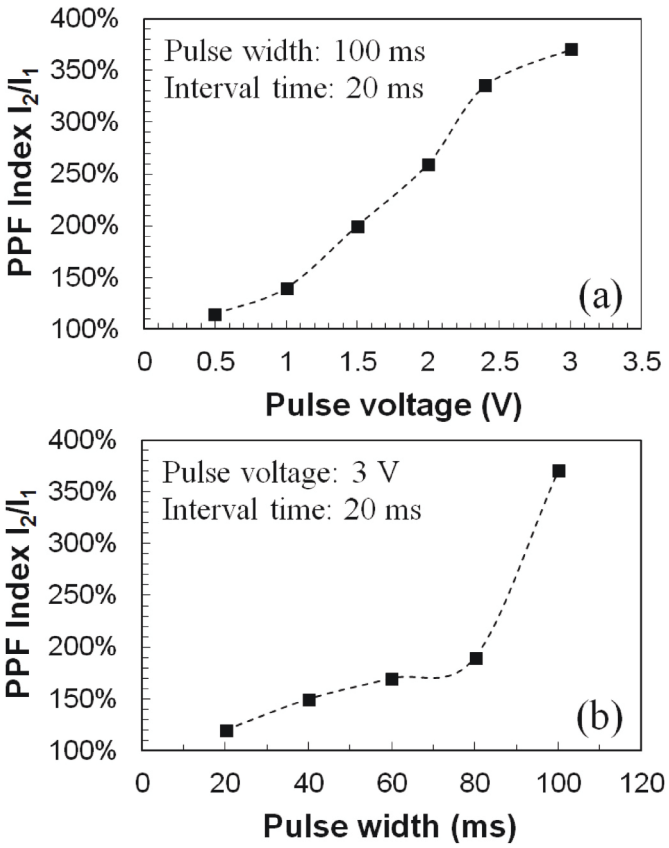

Fig. 8. The PPF index of Al/honey/ITO (90:8) as a function of (a) pulse voltage magnitude in which the pulse width and pulse interval were fixed at 100 ms and 20 ms, and (b) pulse width in which the pulse voltage magnitude and pulse interval were fixed at 3 V and 20 ms, respectively.

Declaration of competing interest

The authors declare that they have no known competing financial interests or personal relationships that could have appeared to influence the work reported in this paper.

Data availability

Data will be made available on request.

Acknowledgments

Feng Zhao acknowledges the support from National Science Foundation, United States (ECCS-2104976); Zhigang Xiao acknowledges the support from National Science Foundation, United States (ECCS-2105388).

References

[1] O. Leon, Chua, Memristor – the missing circuit element, IEEE Trans. Circ. Theor. 18 (1971) 507–519.
[2] Leon O. Chua, Sung Mo Kang, Memristive devices and systems, Proc. IEEE 64 (1976) 209–223.
[3] Tuo Shi, Rui Wang, Zuheng Wu, Yize Sun, Junjie An, Liu Qi, A review of resistive switching devices: performance improvement, characterization, and applications, Small Structures 2 (2021), 2000109.
[4] Furgan Zahoor, Tun Zainal Azni Zulkifli, Farooq Ahmad Khanday, Resistive random access memory (RRAM): an overview of materials, switching mechanism, performance, multilevel cell (mlc) storage, modeling, and applications, Nanoscale Res. Lett. 15 (90) (2020).

[5] D. Ielmini, Brain-inspired computing with resistive switching memory (RRAM): devices, synapses and neural networks, Microelectron. Eng. 190 (2018) 44–53.
[6] Guangdong Zhou, Bai Sun, Xiaofang Hu, Linfeng Sun, Zhuo Zou, Bo Xiao, Wuke Qiu, Bo Wu, Jie Li, Juanjuan Han, Liping Liao, Cunyun Xu, Gang Xiao, Lihua Xiao, Jianbo Cheng, Shaohui Zheng, Lidan Wang, Qunliang Song, Shukai Duan, Negative photoconductance effect: an extension function of the TiOx-based memristor, Adv. Sci. 8 (2021), 2003765.
[7] Guangdong Zhou, Zhijun Ren, Lidan Wang, Bai Sun, Shukai Duan, Qunliang Song, Artificial and wearable albumen protein memristor arrays with integrated memory logic gate functionality, Mater. Horiz. 6 (2019) 1877–1882.
[8] Bingtao Yan, Dalong Kuang, Wenhua Wang, Yuchen Wang, Bai Sun, Guangdong Zhou, Investigation of multi-photoconductance state induced by light-sensitive defect in TiOx-based memristor, Appl. Phys. Lett. 120 (2022), 253506.
[9] X.C. Xing, M. Chen, Y. Gong, Z.Y. Lv, S.T. Han, Y. Zhou, Building memory devices from biocomposite electronic materials, Sci. Technol. Adv. Mater. 21 (2020) 100–121.
[10] Youngjun Park, Jang-Sik Lee, Artificial synapses with short- and long-term memory for spiking neural networks based on renewable materials, ACS Nano 11 (2017) 8962–8969.
[11] Min-Kyu Kim, Jang-Sik Lee, Short-term plasticity and long-term potentiation in artificial biosynapses with diffusive dynamics, ACS Nano 12 (2018) 1680–1687.
[12] Niloufar Raeis-Hosseini, Youngjun Park, Jang-Sik Lee, Flexible artificial synaptic devices based on collagen from fish protein with spike-timing-dependent plasticity, Adv. Funct. Mater. 28 (2018), 1800553.
[13] Chenyang Shi, Jingjuan Wang, Maria L. Sushko, Qiu Wu, Xiaobing Yan, Xiang Yang Liu, Silk flexible electronics: from *Bombyx mori* silk Ag nanoclusters hybrid materials to mesoscopic memristors and synaptic emulators, Adv. Funct. Mater. 29 (2019), 1904777.
[14] Brandon Sueoka, Kuan Yew Cheong, Feng Zhao, Natural biomaterial honey based resistive switching device for artificial synapse in renewable neuromorphic systems and bioelectronics, Appl. Phys. Lett. 120 (2022), 083301.
[15] Brandon Sueoka, Kuan Yew Cheong, Feng Zhao, Study of synaptic properties of honey thin film for neuromorphic systems, Mater. Lett. 308 (2022), 131169.
[16] P.M. da Silva, C. Gauche, L.V. Gonzaga, A.C.O. Costa, R. Fett, Honey: chemical composition, stability and authenticity, Food Chem. 196 (2016) 309–323.
[17] Linda A. Santschi, Patric K. Stanton, A paired-pulse facilitation analysis of long-term synaptic depression at excitatory synapses in rat hippocampal CA1 and CA3 regions, Brain Res. 962 (2003) 78–91.
[18] M.A. Lampert, Simplified theory of space-charge-limited currents in an insulator with traps, Phys. Rev. 103 (1956) 1648.
[19] Aleksey A. Sivkov, Xing Yuan, Kuan Yew Cheong, Xiangqun Zeng, Feng Zhao, Investigation of honey thin film as a resistive switching material for nonvolatile memories, Mater. Lett. 271 (2020), 127796.
[20] R.S. Zucker, W.G. Regehr, Short-term synaptic plasticity, Annu. Rev. Physiol. 64 (2002) 355–405.
[21] D.V. Buonomano, Decoding temporal information: a model based on short-term synaptic plasticity, J. Neurosci. 20 (2000) 1129–1141.
[22] W.G. Regehr, Short-term presynaptic plasticity, Cold Spring Harbor Perspect. Biol. 4 (2012), a005702.
[23] L.Q. Guo, L.Q. Zhu, J.N. Ding, Y.K. Huang, Paired-pulse facilitation achieved in protonic/electronic hybrid indium gallium zinc oxide synaptic transistors, AIP Adv. 5 (2015), 087112.
[24] M.A. Mukhamedyarov, A.L. Zefirov, A. Palotás, Paired-pulse facilitation of transmitter release at different levels of extracellular calcium concentration, Neurochem. Res. 31 (2006) 1055–1058.
[25] B. Katz, R. Miledi, The role of calcium in neuromuscular facilitation, J. Physiol. 195 (1968) 481–492.
[26] Li Qiang, Guo Li, Qiang Zhu, Jian Ning, Ding, Yu Kai Huang, Paired-pulse facilitation achieved in protonic/electronic hybrid indium gallium zinc oxide synaptic transistors, AIP Adv. 5 (2015), 087112.
[27] S.G. Hu, Y. Liu, T.P. Chen, Z. Liu, Q. Yu, L.J. Deng, Y. Yin, Sumio Hosaka, Appl. Phys. Lett. 102 (2013), 183510.
[28] G.D. Wu, P. Feng, X. Wan, L.Q. Zhu, Y. Shi, Q. Wan, Artificial synaptic devices based on natural chicken albumen coupled electric-double-layer transistors, Sci. Rep. 6 (2016), 23578.